Transient Field-Circuit Coupled Models with Switching Elements for the Simulation of Electric Energy Transducers

Herbert De Gersem, Galina Benderskaya, and Thomas Weiland
Technische Universität Darmstadt, Institut für Theorie Elektromagnetischer Felder
Schloßgartenstraße 8, D-64289 Darmstadt, Germany
degersem@temf.tu-darmstadt.de

***Abstract*—This paper deals with the transient simulation of large, nonlinear magnetoquasistatic field models, monolithically coupled to electric circuits with switching elements.**

Keywords—field-circuit coupling, finite-element method, finite-integration technique, adaptive time integration, switching elements.

I. Introduction

Especially for electrical energy transducers operating in the nonlinear range of the BH-characteristic of ferromagnetic material, a technically relevant simulation necessarily combines a small network model for the driving circuit and a large field model dealing with saturation and eddy-current effects. The voltage drops across the *solid* conductors and the currents through the *stranded* conductors generate a magnetic flux $\widehat{\widehat{\mathbf{b}}} = \mathbf{C}\widehat{\mathbf{a}}$ as described by the magnetoquasistatic formulation

$$\widetilde{\mathbf{C}}\mathbf{M}_\nu\mathbf{C}\widehat{\mathbf{a}} + \mathbf{M}_\kappa\frac{d}{dt}\widehat{\mathbf{a}} - \mathbf{M}_\kappa\mathbf{Q}_{\mathrm{sol}}\mathbf{u}_{\mathrm{tw}} - \mathbf{Q}_{\mathrm{str}}\mathbf{i}_{\mathrm{ln}} = 0 \qquad (1)$$

in terms of the line-integrated magnetic vector potential $\widehat{\mathbf{a}}$, here discretised by the finite-integration technique (FIT) [1], the voltage drops $\mathbf{u}_{\mathrm{tw}}$ across the tree branches (twigs) and the currents $\mathbf{i}_{\mathrm{ln}}$ through the co-tree branches (links). $\mathbf{C}$, $\widetilde{\mathbf{C}}$, $\mathbf{M}_\nu$ and $\mathbf{M}_\kappa$ denote the discrete primary and dual curl operators and the reluctivity and conductivity matrices. The field-circuit coupling is represented by the matrices $\mathbf{Q}_{\mathrm{sol}}$ and $\mathbf{Q}_{\mathrm{str}}$ [2]. The currents $\mathbf{i}_{\mathrm{sol}} = -\mathbf{Q}_{\mathrm{sol}}^T\mathbf{M}_\kappa\frac{d}{dt}\widehat{\mathbf{a}}$ induced in the solid conductors and the voltages $\mathbf{u}_{\mathrm{str}} = \mathbf{Q}_{\mathrm{str}}^T\frac{d}{dt}\widehat{\mathbf{a}}$ induced in the stranded conductors are substituted in the mixed circuit formulation

$$-\begin{bmatrix} \mathbf{Q}_{\mathrm{sol}}^T \\ \mathbf{Q}_{\mathrm{str}}^T \end{bmatrix}\frac{d\widehat{\mathbf{a}}}{dt} + \begin{bmatrix} \mathbf{G}_{\mathrm{tw}} & \mathbf{D} \\ \mathbf{D}^T & -\mathbf{R}_{\mathrm{ln}} \end{bmatrix}\begin{bmatrix} \mathbf{u}_{\mathrm{tw}} \\ \mathbf{u}_{\mathrm{ln}} \end{bmatrix} = \begin{bmatrix} -\tilde{\mathbf{D}}\mathbf{i}_{\mathrm{src}} \\ -\hat{\mathbf{D}}^T\mathbf{u}_{\mathrm{src}} \end{bmatrix} \qquad (2)$$

where $\mathbf{D}$, $\tilde{\mathbf{D}}$ and $\hat{\mathbf{D}}$ are parts of the circuit cut-set matrix, $\mathbf{G}_{\mathrm{tw}}$ and $\mathbf{R}_{\mathrm{ln}}$ are the conductances and resistances of the twigs and links respectively, and $\mathbf{i}_{\mathrm{src}}$ and $\mathbf{u}_{\mathrm{src}}$ denote the currents and voltages of the independent sources [3]. The combination of (1) and (2), the linearisation by e.g. the successive substitution approach, and the discretisation in time, e.g., by the singly diagonal Runge-Kutta method (SDIRK), leads to a symmetric, coupled system of equations.

II. 3D-to-0D or 3D-to-0D Coupling

Commonly, the coupling matrices $\mathbf{Q}_{\mathrm{sol}}$ and $\mathbf{Q}_{\mathrm{str}}$ are constructed such that $\mathbf{M}_\kappa\mathbf{Q}_{\mathrm{sol}}\mathbf{u}_{\mathrm{tw}}$ and $\mathbf{Q}_{\mathrm{str}}\mathbf{i}_{\mathrm{str}}$ correspond to the discrete *source* current distribution in the field model. Then, however, both matrices represent a 3D-to-0D coupling, i.e., they connect every degree of freedom inside the conductors to the circuit. In [4] and [2], it has been shown that the arbitrary gradient component of $\widehat{\mathbf{a}}$ can be exploited to formulate a sparser 2D-to-0D coupling, where $\mathbf{Q}_{\mathrm{sol}}$ and $\mathbf{Q}_{\mathrm{str}}$ couple the primary edges or dual faces of a single conductor cross-section to the circuit. Then, $\mathbf{M}_\kappa\mathbf{Q}_{\mathrm{sol}}\mathbf{u}_{\mathrm{tw}}$ and $\mathbf{Q}_{\mathrm{str}}\mathbf{i}_{\mathrm{str}}$ are not free of divergence and can no longer be interpreted as source currents. Moreover, they exhibit a sharp transition, corresponding to a discontinuity of their continuous counterparts, which has to be alleviated by the $-\mathbf{M}_\kappa\frac{d}{dt}\widehat{\mathbf{a}}$ term in the formulation during the solving phase. As a consequence, the condition of the systems of equations is substantially worse. The 2D-to-0D coupling, however, still outperforms the 3D-to-0D coupling because of its higher sparsity [2].

III. Specialised Conductor Models

A stranded conductor is a model for a wire winding with a wire diameter smaller than the skin depth. The eddy-current effects are neglected by omitting $\mathbf{M}_\kappa$ in (1) (3D-to-0D coupling) or by considering an anisotropic conductivity matrix (2D-to-0D case). For particular coil geometries, dedicated models such as, e.g., a foil-winding model, can be inserted in the coupled field-circuit formulation [5].

IV. Adaptive Time-Step Selection

For the case of higher-order time integrators, several solutions of different order of approximation are available. Two of them are used for estimating the error, for deciding whether to accept or to reject the time step and for predicting the new time-step length. In the case of sinusoidal excitations, as is typical for electrotechnical applications, the commonly used solution with an order difference of 1 may fail [6]. This phenomenon is related to the failing even derivatives in the Taylor series for the sine function. A more reliable adaptive time-step selection is achieved when solutions with two orders of difference are used, e.g., the SDIRK-3(1) integrator with a main solution of third order and an embedded solution of first order.

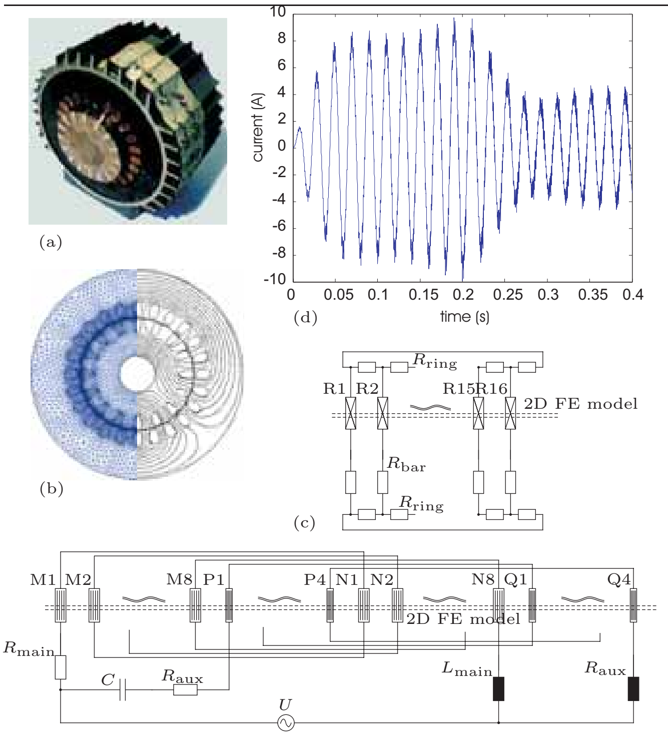

Fig. 1. Capacitor motor: (a) photograph; (b) finite-element mesh and magnetic flux lines at no-load operation; (c) external circuit with the applied sinusoidal voltage U, the capacitance C, the resistances R_{main} and R_{aux} and inductances L_{main} and L_{aux} modelling the end winding parts and the resistances R_{bar} and R_{ring} modelling the rotor ring and rotor-bar parts outside the finite-element model; (d) current through the main stator winding during start-up.

V. Time-Integration over Discontinuities

When field effects due to the switching of power electronic components are considered, the switching events have to be resolved by the time integrator. A next time step is computed under the assumption that no switching happens. Afterwards, a possible event is detected by a sign checking procedure in the case of a θ-type time integrator [7] or by evaluating Sturm sequences in the case of higher-order time integrators [3]. The time step is reduced to the instant of switching, new, consistent begin conditions are computed and the time integration is restarted with a changed circuit [8]. In our implementation, we favour to change the topology of the circuit, and by that, also the structure and possibly also the size of the system matrix, instead of the approach where switches are modelled by highly nonlinear resistors, causing bad condition numbers of the systems of equations [7], [9].

VI. Examples

The first example is a single-phase machine with a start/run capacitor (Fig. 1). Its 2D cross-section is discretised by a finite-element method, resolves local saturation and eddy-current effects by adaptive mesh refinement and models rotor motion by a sliding-surface technique. By transient simulation, the currents through the main and auxiliary windings at start-up are computed. The second example is a three-phase transformer of which the primary side is connected to the grid and the second side is connected to a diode rectifier with an inductive load (Fig. 2). The detection and treatment of switching instants is carried out by a modified SDIRK-3(2) time integrator.

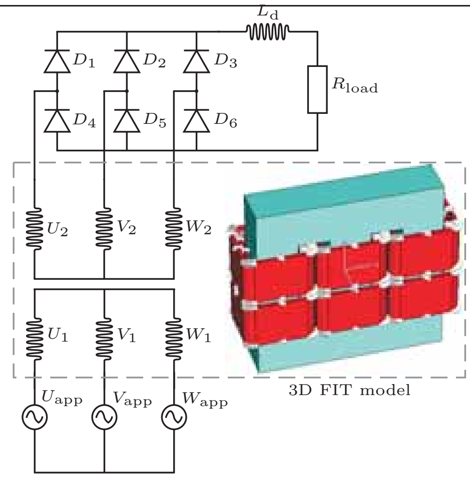

Fig. 2. 3D finite-integration model of a three-phase transformer connected to an external electric circuit for the power grid, diode rectifier and inductive load.

Acknowledgment

The work of H. De Gersem is supported by the Gesellschaft für Schwerionenforschung, Darmstadt, Germany. G. Benderskaya is supported by the Computational Engineering Research Center at the Technische Universität Darmstadt.

References

[1] M. Clemens and T. Weiland, “Transient eddy-current calculation with the FI-method,” *IEEE Trans. Magn.*, vol. 35, no. 3, pp. 1163–1166, May 1999.

[2] H. De Gersem and T. Weiland, “Field-circuit coupling for time-harmonic models discretized by the finite integration technique,” *IEEE Trans. Magn.*, vol. 40, no. 2, pp. 1334–1337, Mar. 2004.

[3] G. Benderskaya, M. Clemens, H. De Gersem, and T. Weiland, “Embedded Runge-Kutta methods for field-circuit coupled problems with switching elements,” *IEEE Trans. Magn.*, vol. 41, no. 5, pp. 1612–1615, May 2005.

[4] P. Dular and J. Gyselinck, “Modeling of 3-D stranded inductors with the magnetic vector potential formulation and spatially dependent turn voltages of reduced support,” *IEEE Trans. Magn.*, vol. 40, no. 2, pp. 1298–1301, Mar. 2004.

[5] H. De Gersem and K. Hameyer, “A finite element model for foil winding simulation,” *IEEE Trans. Magn.*, vol. 37, no. 5, pp. 3427–3432, Sept. 2001.

[6] G. Benderskaya, H. De Gersem, and T. Weiland, “Adaptive time integration for electromagnetic models with sinusoidal excitation,” accepted for presentation at the International Workshop on Electric and Magnetic Fields (EMF06).

[7] P. Dular and P. Kuo-Peng, “An efficient time discretization procedure for finite element-electronic circuit equation coupling,” *COMPEL*, vol. 21, no. 2, pp. 274285, 2002.

[8] G. Mao and L.R. Petzold, “Efficient integration over discontinuities for differential-algebraic systems,” *Comput. Math. Appl.*, vol. 43, pp. 65–79, 2002.

[9] N. Sadowski, B. Carly, Y. Lefevre, M. Lajoie-Mazenc, and S. Astier, “Finite element simulation of electrical motors fed by current inverters,” *IEEE Trans. Magn.*, vol. 29, no. 2, pp. 1683–1688, Mar. 1993.